JJMIE

Volume 19, Number 4, Dec. 2025
ISSN 1995-6665
Pages 795– 805
https://doi.org/10.59038/jjmie/190409
Editor-in-Chief: Prof. Faris M. AL-Oqla

Jordan Journal of Mechanical and Industrial Engineering

Investigation of Mechanical Behavior in Plasma NitridedNickel-Boron-CNT Composite Coatings Using Response Surface Methodology

Alaa Mohammed Hussein Wais[1,*] , Ahlam Hamid Jasim[2]

[1]*Biomedical Engineering Department, College of Engineering, Al-Mustaqbal University, 51001 Hillah, Babil, Iraq.*
[2]*Water Resources Management Engineering Department ,College of Engineering ,Al –Qasim, Green University , Babylon 51013,Iraq*

Received 2 July 2025 *Accepted 20 September 2025*

Abstract

The objective of this study was to statistically analyze the effects of plasma nitriding using response surface methodology(RSM). The RSM, which is dependent on a core composite construction, was used to study the effects of variables like percentage nitrogen / hydrogen flow, deposition time, deposition temperature, and CNT concentration, on wear and corrosion behavior for electroless (Nickel-Boron-CNT)coating for low steel alloy. The results for plasma samples with different CNT concentration (0%, 0.35%, 0.7%) showed the effects of deposition temperature and time as well as percent hydrogen/nitrogen ratio on the corrosion rate. The results of microhardness showed that the highest microhardness value of (1200 HV) was achieved for the Ni-B coating containing 0.35 g/L CNT after plasma nitriding. The optimum design point for plasma nitriding (low wear rate, low friction coefficient, and extreme hardness) was achieved with a desirability of 0.95 at a temperature of 413.03°C for 4h with H2/N2 percentage ratio of %54.17/%45.83 and a concentration of 0.35% CNT, whereas the lowest corrosion rate was achieved at a temperature of 387.78°C for 2.53 h, with H2/N2 percentage ratio of 52.74/47.26 and at a concentration of 0.35g/l CNT. This effect was amplified by raising the deposition temperature between 400 0C and 450 0C. Excellent corrosion resistance is exhibited by the Ni-B-CNT composite coating, and this resistance greatly increases as the concentration of CNTs increases. Excessive CNT deposition leads to agglomeration, harming the coating and reducing its corrosion resistance.

Keywords: RSM, corrosion, plasma nitriding, microhardness.

1. Introduction

Due to its many benefits, aqueous solution electroplating which encompasses both electroplating and electroless plating has garnered a lot of attention lately. These include consistent coating layer preparation, low cost, simplicity of use, high rates of deposition, and promising outcomes like high resistance to wear. It has strong corrosion resistance and high hardness [1]. Electroless nickel plating has changed significantly since, becoming a more well-known method than metal deposition in aqueous solutions. Among the unique characteristics of this technology are amorphous and/or microcrystalline deposits, high reflectivity, abrasion resistance, uniformly high hardness, thickness, good solderability, and remarkable corrosion resistance. Electroless coatings have a wide range of uses, such as bacterial adhesion reduction, heat exchangers, reactor membranes, MEMS, EMI, and powder metallurgy [2-4]. After the Ni-B electroless plating process reached a mature, scalable, and repeatable state, it was made available for mass production in 1989. A method that has drawn a lot of interest for enhancing the surface quality of different substrates is electroless Ni-B plating [5,6]. In many industries, electroless Ni-B plating technology is generally regarded as more appealing and superior to Ni-P plating technology [7]. Not much research has been done on vacuum heat treatment of Ni-B [8]. It is becoming more and more crucial to enhance the mechanical qualities, resistance to corrosion and wear, and coating with nanocomposite materials. It was discovered that additional solid lubricants such as MoS2 [9], Ni-P-CNT [10], CuCNT[11], and PTFE [12] were appropriate for coating nanocomposite materials and widely used in Marine applications, aerospace industry, mechanical engineering and tooling and electronics manufacturing. The use of statistical design techniques like RSM is appealing because it requires fewer experimental runs to determine the relationship between deposition parameters and properties [13]. Study of plasma nitriding parameters (like percentage nitrogen / hydrogen flow, deposition time, deposition temperature, and CNT concentration) on the microstructure, corrosion, and microhardness of low-alloy steels are examined experimentally and statistically in this work in order to enhance the substrate properties.

* Corresponding author e-mail: alaa.mohammed@uomus.edu.iq.

2. Materials and Methods

2.1. Statistical experiment

RSM was employed to identify the optimal conditions, which included the maximum hardness and corrosion rate. Consequently, it also included a number of parameters (CNT concentration, the duration of the CNT deposition process, temperature deposition and the percentage of nitrogen and hydrogen flow). In addition to estimating the effects of each parameter separately and in relation to each response variable, response surface methodology can be used to define the relationships between responses and parameters [14, 15]. Design Expert v10.0 was used for the review of the work as employed in statistical research. CCD stands for central composite design. There were thirty plasma nitriding experiments conducted. Table 1 lists the control values for process parameters. Table 2 includes corresponding design combinations and experimental results for plasma nitriding

Table 1. parameters and the variety of variations.

Parameter	Area of Difference
Time(hour)	1,2,3,4
CNTs (%)	0,0.35,0.7
Temp. (^{0}C)	350-400-450
Hydrogen /Nitrogen flow(sccm)	(25%nitrogen /75%hydrogen, 50%nitrogen/50%hydrogen and75%nitrogen/25%hydrogen)

Table 2. corresponding design combinations and experimental results for plasma nitriding.

Experiment ID	A:Duration (hrs)	B:CNT Content (wt.%)	C:Gas Mixture Ratio (H_2/N_2, sccm)	D:Process Temperature (°C)	Microhardness (HV)	Wear Rate (10^{-4} $mm^3/N{\cdot}m$)	Friction Coefficient	Corrosion Resistance (mpy)
1	4	0.7	75/25	350	690	2.5	0.77	4.4
2	4	0	75/25	350	770	2.2	0.84	4.49
3	1	0.7	75/25	350	615	7.5	1.4	4.2
4	1	0.7	75/25	450	691	7.4	1.4	6.69
5	2.5	0.35	50/50	450	1150	1.2	0.34	0.04
6	1	0.7	25/75	350	610	6.8	1.39	3.69
7	2.5	0.35	50/50	400	1190	0.06	0.31	0.019
8	1	0	75/25	450	730	7.2	1.08	8.39
9	2.5	0	50/50	400	790	0.8	0.61	0.99
10	4	0.7	25/75	350	636	3.2	0.78	6.9
11	4	0	75/25	450	750	2.4	0.8	3.6
12	2.50	0.35	50/50	400.00	1190	0.059	0.30	0.021
13	2.50	0.35	25/75	400.00	1100	0.055	0.33	0.02
14	2.50	0.35	50/50	400.00	1196	0.0599	0.33	0.021
15	2.50	0.35	50/50	400.00	1170	0.02	0.31	0.02
16	2.50	0.70	50/50	400.00	780	1	0.75	0.9
17	4.00	0.70	75/25	450.00	770	2.8	0.7	6
18	2.50	0.35	50/50	350.00	1066	0.5	0.34	0.048
19	1.00	0.35	50/50	400.00	1110	3.8	0.6	1.9
20	4.00	0.00	25/75	350.00	675	3.5	0.8	4.8
21	1.00	0.00	75/25	350.00	780	7.1	1.38	7
22	2.50	0.35	75/25	400.00	1100	0.3	0.36	0.02
23	4.00	0.70	25/75	450.00	750	2.2	0.8	4
24	4.00	0.00	25/75	450.00	750	2.8	0.8	2.13
25	2.50	0.35	50/50	400.00	1190	0.25	0.3	0.02
26	1.00	0.00	25/75	350.00	680	7.4	1.34	6
27	4.00	0.35	50/50	400.00	1250	0.01	0.21	0.6
28	1.00	0.70	25/75	450.00	600	7	1.45	3.59
29	2.50	0.35	50/50	400.00	1143	0.52	0.41	0.85
30	1.00	0.00	25/75	450.00	765	7.5	1.35	6

2.2. Preparation of the substrate

4340 steel was the substrate metal utilized in this article. Samples with dimensions of 20 mm in diameter and 10 mm in height made up the substrate. Table 3 shows the results of the chemical analysis of 4340 steel.

Table 3. Chemical analysis of steel AISI 4340.

Element	C	Si	Ni	S	Mn	P	Cr	Mo	Fe
Weight Percentage (%)	0.3	0.3	1.3	0.005	0.7	0.009	0.80	0.15	Bal.

Every sample was ground and polished. One minute was spent submerging the materials (30 g/L NaOH, 60 g/L NaCO3, and 60 g/L NaPbO4) in a solution at 70 °C. To get rid of any oil from the metal surface, the electrolyte was magnetically stirred using a power source (5 volts).

2.3. CNT Ball-Milling

US Nanomaterials Research, Inc. supplied MWCNTs with an overall purity of over 95%, an outer diameter of 20–30 nm, and an inner diameter of 5-10 nm. Figure 1 displays images of the CNTs both before and after they were ball milled. The distribution of carbon nanotubes in the metallic matrix phase of an electroless Ni-B coating is essential for maintaining a stable and homogeneous dispersion and avoiding agglomeration. Before being combined with CNTs, SDS (sodium dodecyl sulfate) surfactants were combined with water for 45 minutes using an ultrasonic device.

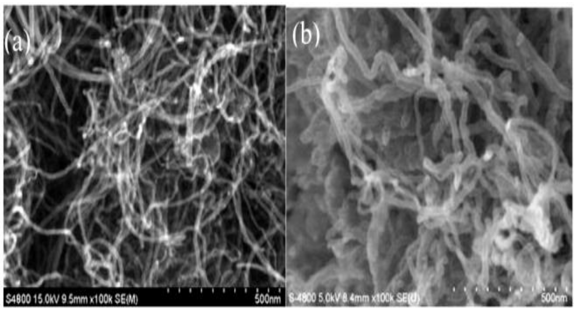

Figure 1. Images FESEM of ball milled and as-received carbon nanotubes.

2.4. Preparation of the Electroless Bath

Following surface preparation, the electroless plating bath was made using the concentrations listed in Table 4. The Ni-B coating was applied to the substrate using a coating procedure. The coating bath's pH ranged from 12 to 14. At 95 ± 1 °C, the electroless Ni-B coatings were applied for an hour. During coating, a magnetic stirrer was used to mix the bath solution, which lessened ion concentration variations. Every ten minutes, a sample was taken from a monastery to guarantee a consistent layer thickness. Two distinct CNT concentrations (0.35- 0.7g/l) were used when the Ni-B-CNT coating was applied show in Figure 2.

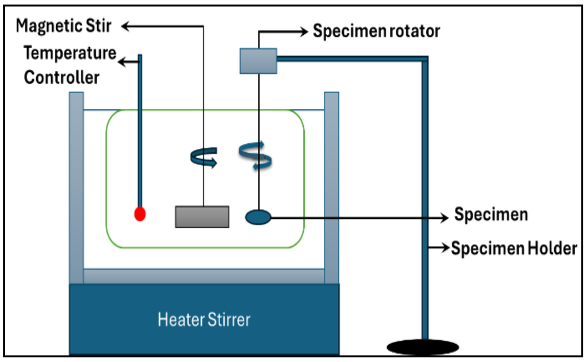

Figure 2. Electroless deposition process setup in an experiment.

Table 4. Conditions electroless bath operates.

Composition of Bath	Quantity
Nickel chloride	20 g/l
Sodium borohydride	0.7g/l
Ethylenediamine	50 ml/l
Lead Nitrate	0.01 g/l
Sodium hydroxide	85 g/l
Sodium Dodecyl Sulfate	0.1 g/l
Carbon nanotube	0, 0.35, 0.7 g/l
Operating conditions	
pH	13
Temperature	95 ^{0}C
Time of immersion	1 hour

2.5. Plasma Nitriding Treatment

Table (5) displayed the working conditions for the electroless bath nitriding treatments.

Table 5. Plasma nitriding treatment operating conditions.

Conditions	Pluse DC Plasma Nitriding (PPN)
Temp. (^{0}C)	350ºC ,400 ºC,450ºC
Pressure	10 $^{-2}$ torr
discharge voltage	400-500 V
Frequency	8.9 kHz
Duty cycle	70%
Current(A)	2-3
Gas composition	25%nitrogen/75%hydrogen, 50%nitrogen/50%hydrogen and75% nitrogen/25%hydrogen
Duration (hour)	1,2,3,4

2.6. Characterization

A Vickers hardness was employed to measure the coating layers' microhardness under a 25 g load for 15 seconds. The panel extrapolation technique was used to assess the coatings' corrosion behavior. The corrosion potential (Ecorr) is the voltage differential between a sample submerged and a reference electrode. Current density of corrosion (icorr). and coatings that gauge the rate of corrosion in a solution of 3-5% NaCl. The crystalline phase of the coatings was ascertained through analysis. The plating phase was identified using (XRD), and the samples' crystal structure was ascertained.

3. Results and Discussion

3.1. Surface morphology.

The morphology for the surface coating of the sample was depicted in Figure 3, while Figure 3a displays the Ni-B sample's smooth, cauliflower-like microstructure. Lubricants exposed to adhesive wear conditions might benefit from this structure [16, 17]. While a smaller proportion of CNTs protruded from the coated surface, the majority of CNTs were found to be fixed in the matrix by particle dispersion. On the other hand, as Figure 3b illustrates, CNTs were discovered on the sample's surface with 0.35 g/L CNTs. Additionally, there was a significant shift in the microstructure of the sample containing 0.35 g/L CNTs. This observation makes sense because CNTs can fill in gaps and cracks due to their low concentration, increasing the surface area that is uniformly coated. The degree of nodule growth increased as the CNT concentration was raised to 0.7 g/L in Figure 3c. Because of their high concentration, large particles were the cause of the observed CNT aggregation around the Ni-B-0.7 g/L CNT sample. Large particles on the sample surfaces start to take on shapes linked to Ni nucleation during CNT agglomeration because of the CNTs' aggregation on the base metal. A higher magnification image of the sample is also displayed in Figure 3d to further emphasize the CNT distribution.

FESEM analysis conducted on plasma-nitrided specimens revealed reveal a change in Ni-B morphology toward a microstructure resembling cauliflower, as seen in Figure (4a). It is widely acknowledged that the observed structure results from perfect deposition at the initial locations of surface defects [18,19]. Figure (4b) displays a sample with a similar density of 0.35 g/L CNTs. Since the crystals first form at different preferred locations, Ni2B, Ni3B, and BN particles actually collide on the sample surface. Additionally, atom re-deposition, sputtering, and plasma nitriding treatment can be used to redeploy compounds to fill gaps. The sample containing 0.7 g/L CNTs had coarser particles, as seen in Figure (4c). The size of the agglomerated particles increases due to the high concentration of CNTs following plasma nitriding treatment, which may hasten the nucleation growth of the nanoclusters in this sample. However, no CNT is visible on the surface of the sample. As a result of plasma nitriding, a solid ion bombardment eliminates an excessive number of carbon nanotubes on the top surface.

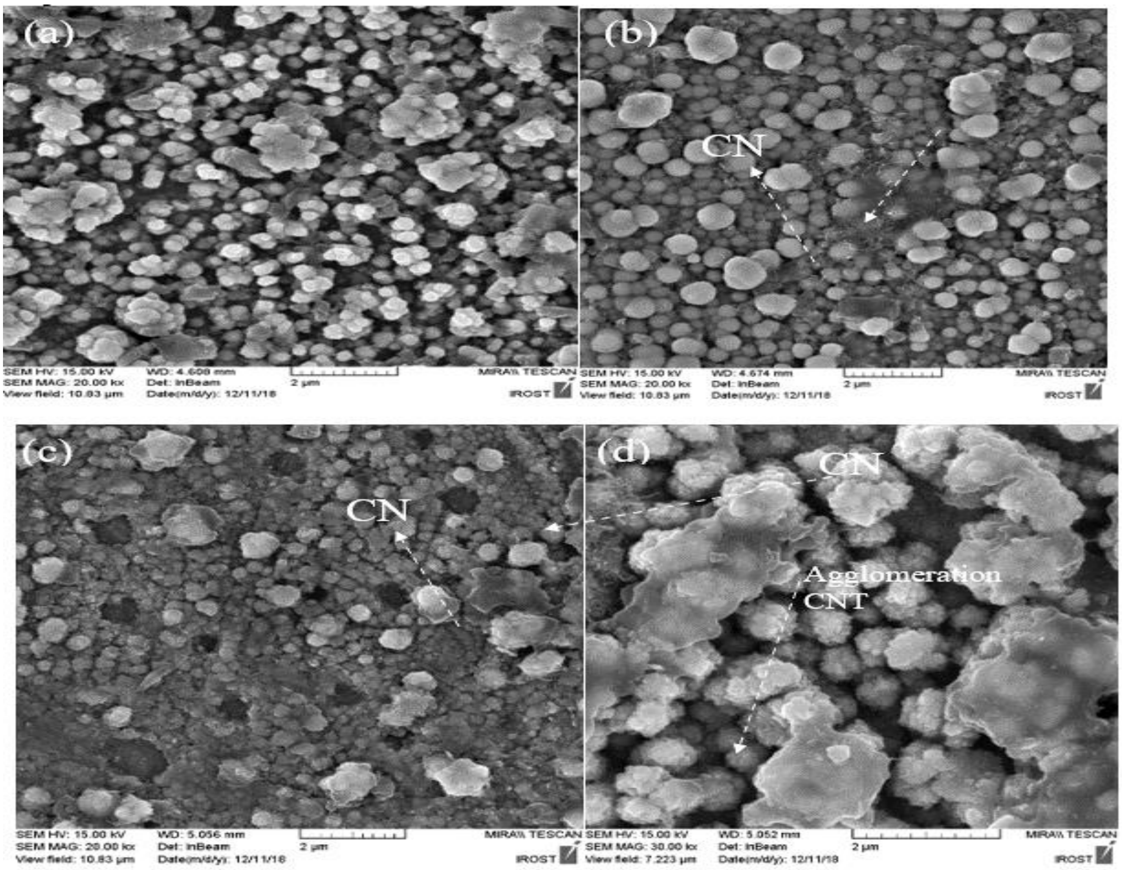

Figure 3. Images FESEM of the samples that were coating with (a) Nickel-Boron, (b) Nickel-Boron composite containing 0.35 g/L carbon nanotubes, (c) Nickel-Boron composite with 0.7 g/L carbon nanotubes, and (d) Nickel-Boron composite reinforced with 0.7 g/L CNTs.

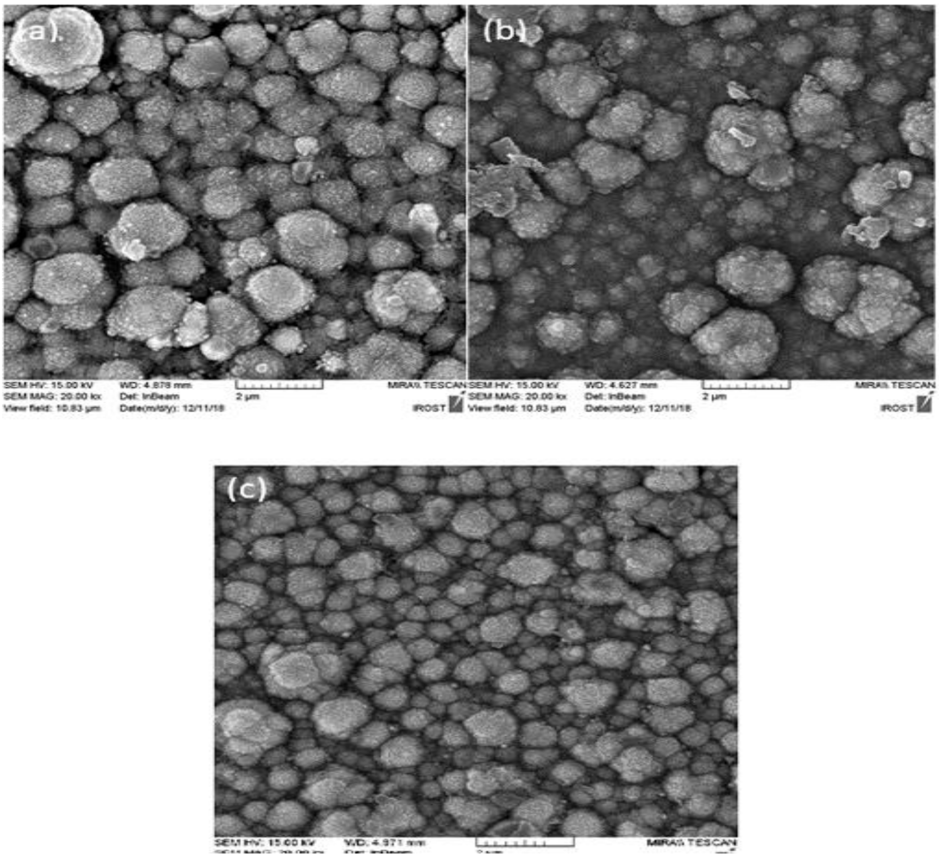

Figure 4. FESEM (a) Nickel-Boron, (b) Nickel-Boron with 0.35 grams per liter of carbon nanotubes, and (c) Nickel-Boron with 0.7 grams per liter of carbon nanotubes plasma nitride.

3.2. XRD

Figure 5 displays a Ni-B coating's X-ray diffraction (XRD) patterns. The electroless deposited Ni-B coating exhibits a peak in this pattern, suggesting an amorphous structure. It is widely acknowledged that amorphous elements, like boron(B), prevent the nucleation of nickel(Ni) [20]. Peak broadening is decreased when carbon nanotubes (CNTs) are added to the electroless bath; a sharper peak is produced when the concentration of CNTs increases. This implies that Ni functions as a nucleation site in CNT crystals, giving Ni-B CNTs a more semicrystalline microstructure [20]. The formation of intermetallic compounds, Ni2B and Ni3B, following plasma nitriding treatment causes the treated samples to change from an amorphous to a crystalline microstructure, as shown in Figure 6. The unstable Ni2B phase breaks down to produce the Ni3B phase. Furthermore, continuous exposure to positively charged ions can raise the sample's surface temperature, which will promote the development of the Ni2B and Ni3B phases. It is generally acknowledged that the microstructure of boron nitride (BN) is responsible for the observed peak in each sample [20]. Active nitrogen and boron atoms in the plasma environment combine during sputtering to create BN.

3.3. Data analysis via RSM

Design Expert software was used to examine the correlations between the experimental parameters (deposition temperature, CNT concentration, time deposition, and percentage N and H flow) and the responses (the rate of wear, coefficient of friction, corrosion rate and hardness). Two essential phases in the modeling process are choosing a suitable model and proving its efficacy [21-23]. The F test and P value were used to assess the significance of a number of models, including two-factorial, linear, cubic, and quadratic. The findings showed that a quadratic model effectively captured the relationships between the parameters (corrosion rate and hardness) for specimens that underwent plasma nitriding (Tables 6-9).The friction coefficient decreases as the CNT concentration increases up to 0.35 g/L. This reduction can be attributed to the easy shear and rolling action of the carbon-based lubricating film.Excellent corrosion resistance is exhibited by the Ni-B-CNT composite coating, and this resistance greatly increases as the concentration of CNTs increases. Excessive CNT deposition leads to agglomeration, harming the coating and reducing its corrosion resistance.

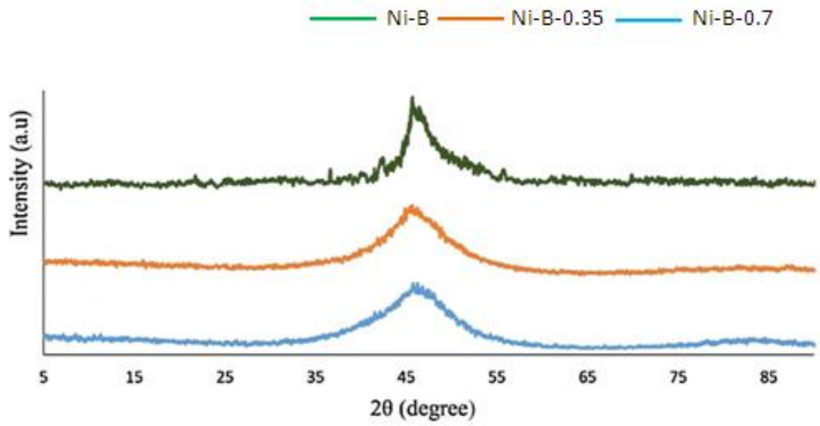

Figure 5. XRD analysis of Nickel-Boron and Nickel-Boron reinforced with CNTs plated samples

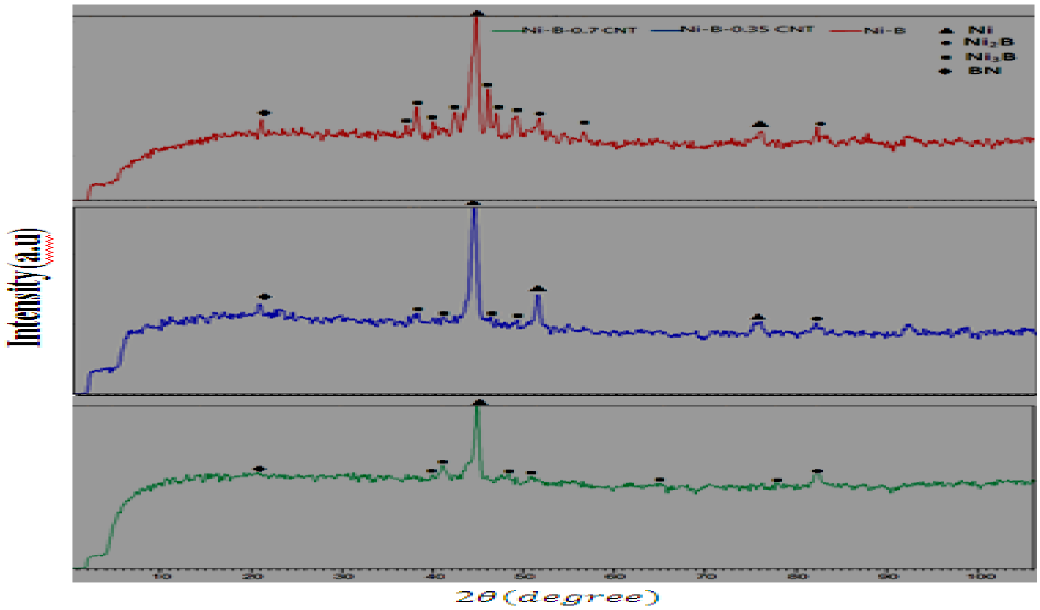

Figure 6. XRD analysis of Nickel-Boron and Nickel-Boron reinforced with CNTs plasma nitriding samples

Table 6. Summary of Wear Rate Analysis for Plasma-Nitrided Samples.

Model Type	P-Value	P-Value (lack of fitness)	Statistic (F)	
linear	0.016	< 0.0001	198.80	
Two-Factor Interaction (2FI)	0.9978	< 0.0001	280.9	
quadratic	< 0.0001	0.0480	4.8	Recommended
cubic	0.5	0.0169	9.9	Confounded (Alias)

Table 7. Summary of Coefficient of friction Analysis for Plasma-Nitrided

Model Type	P-Value	(lack of fitness)P-Value	Statistic (F)	
linear	0.0922	< 0.0001	109.40	
Two-Factor Interaction (2FI)	0.9996	< 0.0001	153.9	
Quadratic	< 0.0001	0.0689	4.02	Recommended
Cubic	0.5395	0.0252	8.40	Confounded (Alias)

Table 8. The plasma nitriding samples' hardness.

Model Type	P-Value	(lack of fitness)P-Value	Statistic (F)	
linear	0.9999	< 0.0001	255.23	
Two-Factor Interaction (2FI)	0. 9402	< 0.0001	180.19	
Quadratic	< 0. 001	0.07	3.9	Recommended
Cubic	0. 136	0. 10	3.7	Confounded (Alias)

Table 9. Summary for the corrosion rate fit for samples submitted to plasma nitriding.

Model Type	P-Value	(lack of fitness)P-Value	Statistic (F)	
2F1	0.7657	< 0.0001	107.56	
Linear	0.8724	< 0.0001	88.35	
quadratic	< 0.001	0.0493	4.77	Recommended
cubic	0.8316	0.0084	14.40	Confounded (Alias)

The significance of the selected model is investigated using an analysis of variance, or ANOVA. Tables (10-13) display the ANOVA results. The "last-of-fit" test is used to assess the model's effectiveness. The findings imply that a quadratic model chosen for the sample's wear rate, microhardness and friction coefficient, for plasma nitriding has a small "misfit.". With a F value of 193.60, the quadratic model selected for the wear rate was significant. The likelihood of noise producing a model value of F is a mere 0.01%

Table 10. Statistical analysis of wear rate through ANOVA for plasma-nitrided samples

Factor	P-value	Statistic(F)	Probability (P> F)	
(quadratic)	Model Type	193.60	< 0.0001	Statistically insignificant
	Lack of fit	4.48	0.0532	Not Statistically insignificant
R^2=98.87% Adj R^2=98.35%				

Table 11. Analysis of Variance (ANOVA) results for the friction coefficient in plasma-nitrided specimens

Factor	P-value	F-statistic	Probability (p > F)	
Quadratic	Model	110	< 0.0001	Statistically insignificant
	Lackoffit	3.3	0.0991	Not statistically insignificant
R^2=98.30% AdjR^2=97.41%				

Table 12. Analysis of Variance (ANOVA) results for hardness in plasma-nitrided specimens.

Factor	p-value	Statistic(F)	Probability (p > F)	
Quadratic	Lack-of-fit test	3.49	0.079	Not Statistically insignificant
	Model type	156.47	< 0.0001	Statistically significant
AdjR^2=97.9% R^2=98.1 %				

Table 13. ANOVA findings of the plasma nitriding s corrosion rates samples'.

Factor	P-value	Statistic F	P- value of P >F	
quadratic	Model	42.92	< 0.0001	Statistically significant
	lack of fit	4.53	0.0533	Not statistically significant
Adj R^2=94% R^2=96.7%				

Several parameters exhibited p-values greater than 0.05were eliminated from the equations based on the ANOVA results. The models' ANOVA indicates that these terms are not significant. Backwards, unnecessary terms are removed. The following list of response equations is the result of applying a "multiple regression analysis" to the experimental data after the non-significant terms have been eliminated.

1. The final fitted model representing the wear rate of plasma nitrided specimens, based on coded variables, can be expressed as follows:

$$\text{Wear rate}=-0.066-2.23A-0.028B-0.06\,C-0.011D+0.21BC+2.19\,A^2+1.19\,B^2+0.47\,C^2+1.14D^2 \quad (1)$$

Figures (7 a and b) show the influence of temperature and duration on wear rate of plasma nitrided samples was investigated through plotted trends, under constant CNT concentration (0.35%) and a fixed H_2/N_2 gas ratio of 50%.

The graphical results indicate that the wear rate of the samples tends to decrease as both the deposition time and temperature increase from 350 °C to 400 °C. However, an increase in temperature to 450 °C leads to a rise in wear rate. This behavior suggests that wear performance is influenced not only by the testing conditions but also by intrinsic material characteristics, such as surface morphology, hardness, and the coefficient of friction.

2. The developed regression model representing the friction coefficient for plasma-nitrided is presented below, expressed in terms of the coded variables of the process parameters.

$$\text{Coefficient friction}=+0.29-0.27A+0.024B-0.017C-0.019D-0.040AB-0.030CD+0.16A^2+0.43B^2+0.098C^2+0.093\,D^2 \quad (2)$$

Figures (8 a and b) show The plotted results demonstrate the impact of deposition temperature and time on the of friction coefficient plasma nitrided, maintained at a 0.35 CNT g/L and a hydrogen-to-nitrogen ratio of 50%. The friction coefficient is observed to decline as the deposition time increases and the temperature increases from 350 °C to 400 °C.

3. Equation: final equation explains the fitted model of plasma nitriding hardness samples usingcoded factors.

$$\text{Hardness}=+1172+26*A-29.9*B+17.9*C+23.9*D+22*A*B-370*B^2-53*C2-45.9*D^2 \quad (3)$$

Figures 9 a and b illustrate how the temperature and duration of the deposition process affect the hardness of samples plasma nitriding to a constant concentration of carbon nanotubes (0.35 g/L) and with a 50% hydrogen/nitrogen ratio. The figures demonstrate how the samples' hardness rises from 350 °C to 400 °C as the deposition time and temperature increase, and falls from 400 °C to 450 °C as the deposition temperature and time increase.

4. The equation provides an explanation of the fitted corrosion rate model for sample plasma nitriding. The final equation in the coded factor terms is as follows:

$$\text{Corrosion rate} =-0.31-0.58A-0.16B+0.42C-0.068D+0.97AB0.41*A*C0.55*A*D+0.65*C*D+1.9*A2+1.73*B2+0.80*C2+0.82*D2 \quad (4)$$

For plasma nitriding samples with a constant carbon nanotube (CNT) concentration and a hydrogen/nitrogen ratio percentage of 50%, Figures (10 a and b) display graphs illustrating the effects of time and temperature on corrosion rate. According to the figures, the samples' corrosion rate decreases when the and deposition time and temperature are increased from 2.5 hours to 4 hours; however, the samples' corrosion rate increases when the deposition temperature is raised from 400 °C to 450°C and the time is increased from 2.5 hours to 4 hours.

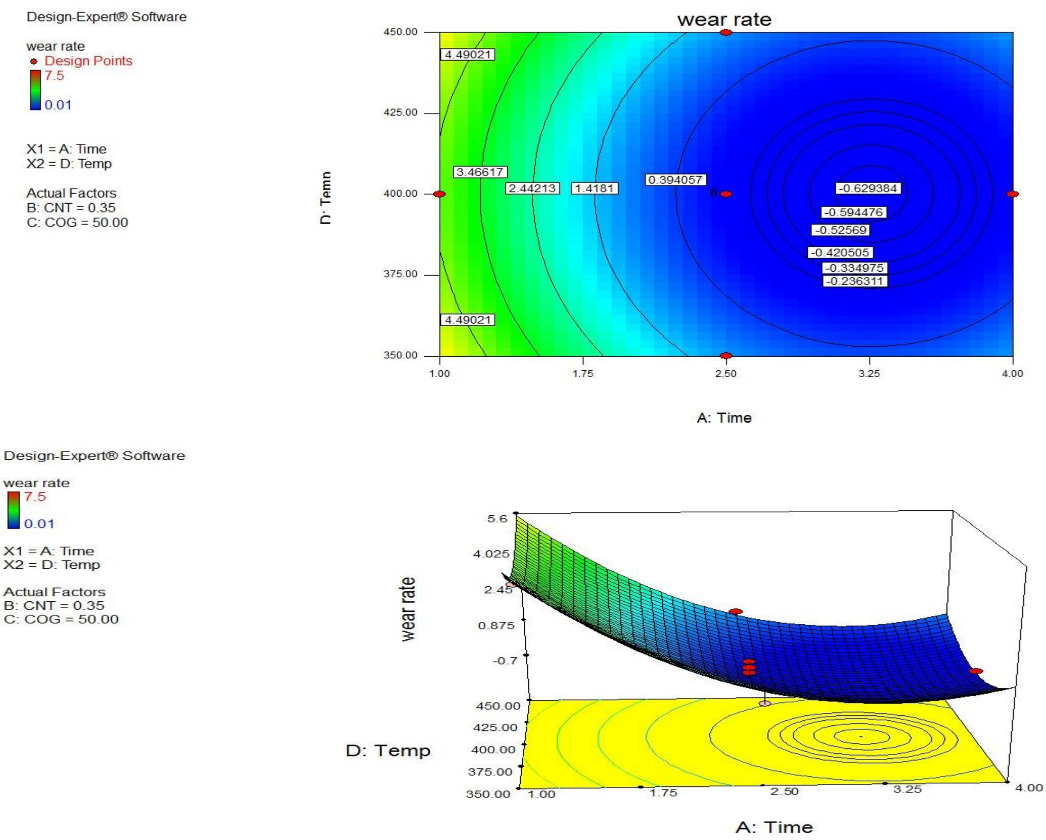

Figure 7. The effect and time and temperature on wear rate for plasma nitrided samplesunder constant CNT concentration (0.35 g/L) and a hydrogen/nitrogen gas ratio of 50%is illustrated through (a) 2D contour plots and (b) 3D surface plots.

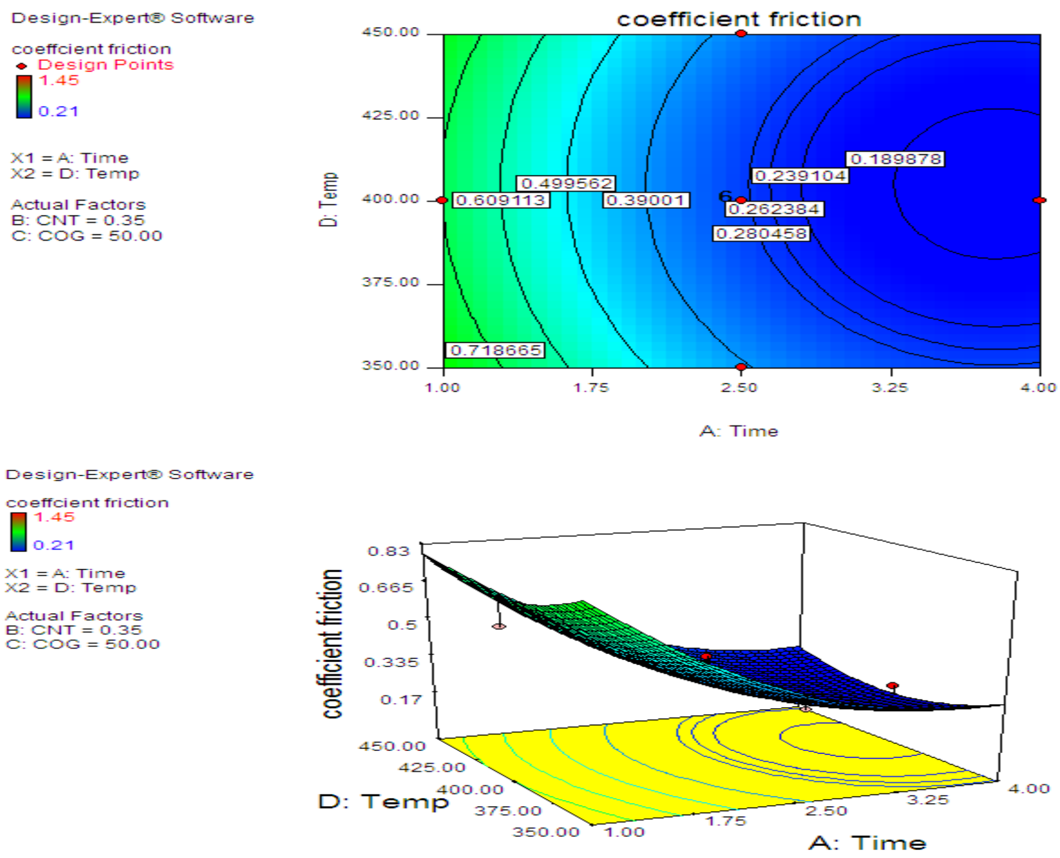

Figure 8. The effect and time and temperature on coefficient of friction of plasma nitrided samples—at a fixed CNT concentration of 0.35 g/L and a hydrogen/nitrogen ratio of 50%are presented using (a) 2D contour plots and (b) 3D surface plots.

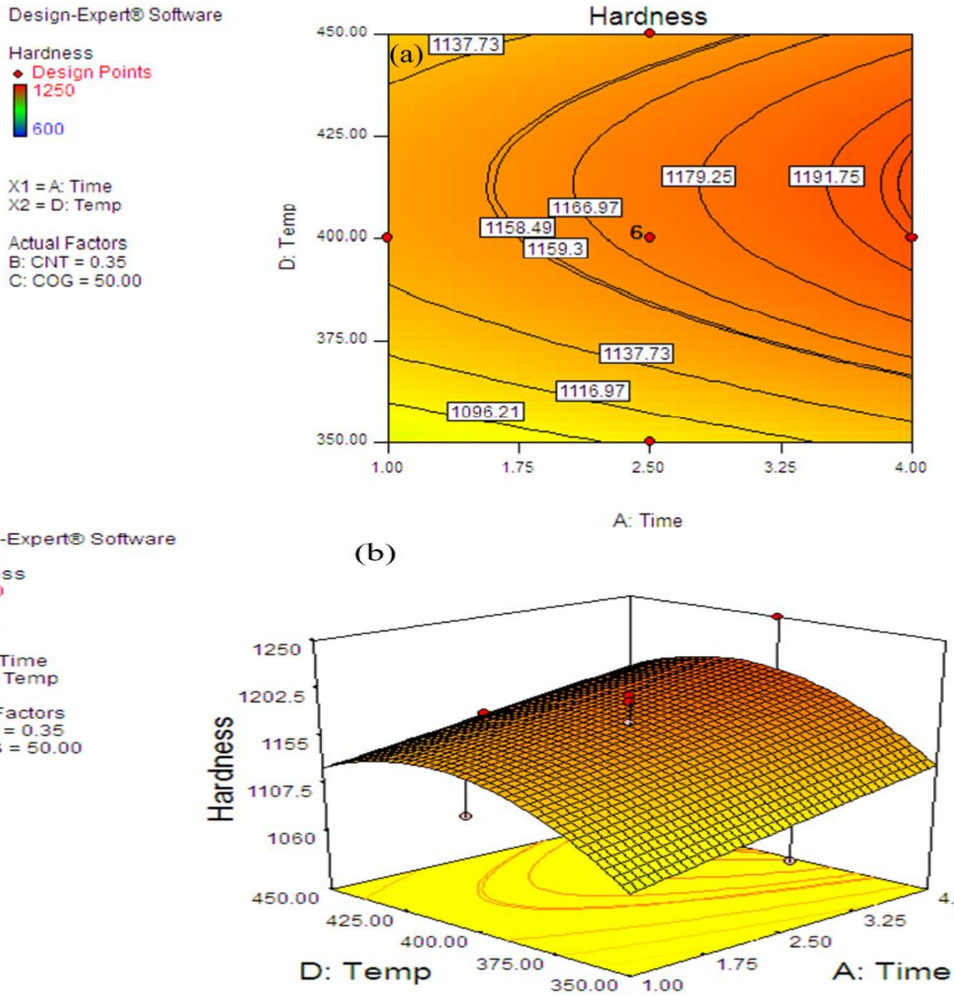

Figure 9. Deposition temperature and time effects on the micohardness of samples exposed to plasma nitriding at constant CNT concentrations (0.35 g/l) and hydrogen/nitrogen ratios (50 percent): (a) 2D contour and (b) 3D surface

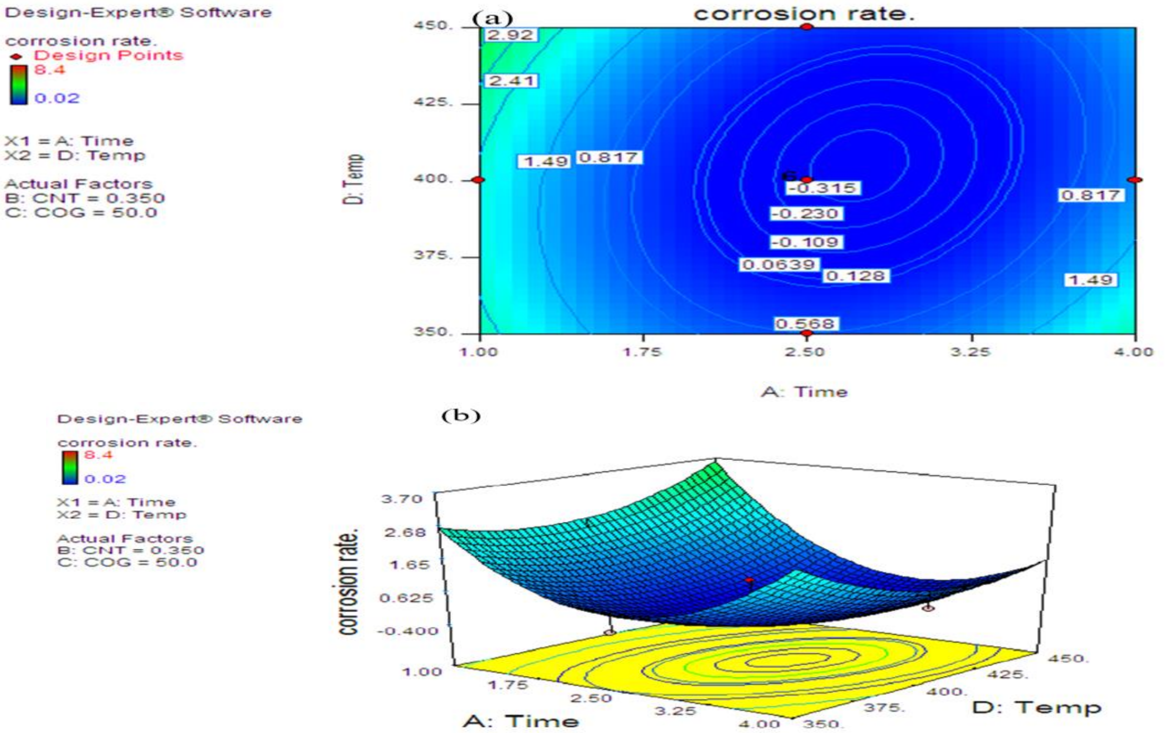

Figure 10. Deposition temperature and time effects on the rate of corrosion exposed to plasma nitriding samples with a constant CNT concentration (0.35 percent) and 50%hydrogen/nitrogen ratio: (a) 2D contour and (b) 3D surface

Table 14 outlines the parameter sets along with the applied constraints used during the optimization procedure. The outcomes of the RSM-based optimization considering the input variables (deposition temperature, deposition time, CNT concentration, and H_2/N_2 gas ratio) and the corresponding responses (wear rate, friction coefficient, hardness, and corrosion rate)are detailed in Table 15.

The optimal design condition, corresponding to a desirability value of 0.9507achieving minimal wear rate and friction coefficient alongside maximum hardness was attained at a deposition temperature of 413.03 °C, a duration of 4 hours, a hydrogen-to-nitrogen ratio of 54.17%/45.83%, and a CNT concentration of 0.35 g/L

, as shown in Figure 10. The optimum design point (the lowest corrosion rate) exhibits the following: temperature (387.78^{0}C), time (2.53 h), percentage hydrogen/nitrogen ratio (52.74/47.26), and concentration of CNT (0.35g/l), as shown in Table (16).

Table14. The process of optimizing the coating electroless sample's plasma nitriding involves the use of parameter groups and constraints.

Parameter	Optimization Goal	Lower Limit	Upper Limit
Temperature (^{0}C)	Within range	350.00	450.00
COG(H_2/N_2)(sccm)	Within range	25.00	75.0
Duration (h)	Within range	1.00	4.00
CNT content (%)	Within range	0.0	0.70
microhardness	Maxi.	600.00	1300.00
Wear rate (mm^3/Nm)	Min.	0.01E-4	7.5 E-4
coefficient of friction	Min.	0.2	1.5
Corrosion rate (mpy)	Mini.	0.02	8.4

Table 15. RSM Optimization Parameters for Plasma Nitriding of Coated on key response variables.

No.	Time (hour)	CNT %	Temp. (^{0}C)	COG(H_2/N_2) (sccm)	Hardness (HV)	Specific rate of wear (mm^3/N m)*10^{-4}	The coefficient of friction	(Desirability)
1	4	0.35	413.03	54.17/45.83	1201.54	-0.022	0.175235	0.9507 suggested
2	3.99	0.39	416.07	55.14/44.86	1201.09	0.0100071	0.176918	0.950

Table 16. The results of (RSM) optimization demonstrated effect of process parameters on rate of the corrosion of plasma-nitridedcoated samples.

Number	Time (hour)	CNT %	Temp. (^{0}C)	COG(H_2/N_2) (sccm)	Corrosion rate (mpy)
1	2.53	0.35	387.78	52.74/47.26	-0.2152 suggested
2	2.94	0.39	420.27	41.20/58.80	-0.324063

4. Conclusion

- An improvement ratio of 245% was found for microhardness, by plasma-nitriding Nickel-Boron-0.35g/l CNT in an atmosphere comprising 50% N2 and 50% H2 and at a temperature of 400°C for 4h.
- An improvement ratio of 99.7% was found for reduction-specific wear rate, which was achieved by plasma nitriding Ni-B-0.35g/l CNT in an atmosphere of 50% N2 and 50% H2 and at a temperature of 400°C for 4h
- The best addition percentage of carbon nanotube to Ni-B coating is(0.35g/l CNT).that coating (Ni-B-0.35 G/LCNT) the friction coefficient decreased to (0.51), decreased to (0.17) after plasma-nitriding of coating electroless (the best condition is 400^{0}C,4 hours and the percentage of gas of hydrogen/nitrogen (50%)).
- The optimum design point for plasma nitriding (low wear rate, low friction coefficient, and extreme hardness) was achieved with a desirability of 0.95 at a temperature of 413.03°C for 4h with H2/N2 percentage ratio of %54.17/%45.83 and a concentration of 0.35% CNT, whereas the lowest corrosion rate was achieved at a temperature of 387.78°C for 2.53 h, with H2/N2 percentage ratio of 52.74/47.26 and at a concentration of 0.35g/l CNT.
- Important change in the microstructure was observed in the specimen containing 0.35g/l of CNTs, which seems logical and leads to increase the uniformly coated surface. The CNTs aggregation that was observed results from the presence of more particles about Ni-B-0.7g/l CNT specimen.

References

[1] Q. Barati, Seyed Mohammad Mehdi Hadavi. “Electroless Ni-B and composite coatings: A critical review on formation mechanism, properties, applications and future trends”. Surfaces and Interfaces Volume 21,2020, 100702.

[2] MuslumYunacti, AlexandreMégret,Mariana Henriette Staia ,Alex Montagne andVéronique Vitry”Characterization of Electroless Nickel–Boron Deposit from Optimized Stabilizer-Free Bath”.Coatings, 2021, 11(5), 576.

[3] Manik Barman1, Tapan Kumar Barman1 and Prasanta Sahoo” Tribological behavior of electroless Ni-B ternary and quaternary coatings with inclusion of W and Mo”. Materials Research Express, Physica Scripta,Volume 99,2023.

[4] Manik Barman, Tapan Kumar Barman, and Prasanta Sahoo, “Effect of heat-treatment temperature and borohydride concentration on corrosion behaviour of ENB coating” .App. Journal of Mechanical Engineering Science, Volume 237, Issue 1,2023, Pages 3-19.

[5] Alaa W, Abdual R K and Farzad M. “Comparing the effect of heat treatment and plasms-nitriding corrosion resistance of Ni-B-CNT elecctroless coating with different CNT concentration on AISI 4340 STEEL”. International Journal of Mechanical and Production Engineering Research and Development (IJMPERD), 2019, 9(5),183-196.

[6] A. H. Jasim, A. R. K. Abidali, A. M. Wais,” Investigating the Effect of Fe2O3 on Wear Behaviour and Corrosion Resistance

of Electroless Ni–P Coating with Different Fe2O3 Concentrations on AISI 4140 Steel" METALS, ALLOYS, COATINGS", 2023, Vol. 29 No. 2.

[7] Véronique Vitry, Abdoul-Fatah Kanta, "Fabienne Delaunois. Mechanical and wear characterization of electroless nickel-boron coatings. Surface and Coatings". Technology Volume 206, Issue 7, 25, 2011, Pages 1879-1885.

[8] He Y, Wang S, Walsh F, Chiu YL and Reed P. "Self-lubricating Ni-P-MoS2 composite coatings",Surf. Coat. Technol.,2016,307, P.P.926-934.

[9] Wang Q, Callisti M, Miranda A, McKay B, Deligkiozi I and Milickovic TK. "Evolution of the structural, mechanical and tribological properties of the Ni-P/MWCNT coatings as a function of the annealing temperature". Surf. Coat. Technol, 2016,302,195-201.

[10] Tsai PC, Jeng YR, Lee JT, Stachiv I and Sittner P. "Effects of carbon nanotube reinforcement and grain size refinement mechanical properties and wear behaviors of carbon nanotube/copper composites".Diam. Relat. Mater.,2017, 74, 197-204.

[11] Wan Y, Yu Y, Cao L, Zhang M and Qi C. "Corrosion and tribological performance of PTFE-coated electroless nickel boron coatings". Surf. Coat. Technol,2016, 307,316-323.

[12] ShaoqiuYan,Ying Tang GangpingBi,BowenXiao,Guotian He, andYuanchang Lin. "Optimal Design of Carbon-Based Polymer Nanocomposites Preparation Based on Response Surface Methodology". Polymers,2023, 15(6), 1494.

[13] Reza T, Farzad M. "Ability of plasma nitriding to improve tribological behavior of mediumand high boron electroless nickel coatings". Tribology International,2021,156: 106822

[14] Bezerra MA, Santelli RE, Oliveira EP, Villar LS, EscaleiraL A. "Response surface methodology(RSM)as a tool for optimization in analytical chemistry". Talant a ,2008, 76, 965–77.

[15] Veronique Vitry, Elodie Francq, and Luiza Bonin. "Mechanical properties of heat-treated duplex electroless nickel coatings". Surface Engineering. Volume 35 Issue 2, February 2019.

[16] Rohit Agrawal. Arkadeb Mukhopadhyay" Inclusion of W in electroless Ni–B coating developed from a stabilizer free bath and investigation of its tribological behavior" Journal of the Indian Chemical Society, Volume 100, Issue 4,2023, 100966.

[17] Mustafa Anik, Erhan Korpe, and Esin Sen. "Effect of coating bath composition on the properties of electroless nickel-boron". lms. Surface and Coatings Technology,Vol. 202,2008, pp.1718-1727.

[18] V. Vitry, L. Bonin, "Formation and characterization of multilayers borohydride and hypophosphite reduced electroless nickel deposits".Electrochim, Acta,Vol. 243,2017, pp. 7-17.

[19] E. Georgiza, V. Gouda, P. Vassiliou, "Production and properties of composite electroless Ni-B-SiC coatings". Surf. Coat. Technol, Vol.325,2017, pp. 46-51.

[20] Ghafari E, Costa H, Júlio E. "RSM-based model to predict the performance of self-compacting UHPC rein forced with hybrid steel microfibers". Constar Build Mater,2014, 66:375–83.

[21] ShahsharifShaikh,MohammadaminSadeghi,Sandra Cruz, and Fábio Ferreir" Recent Progress on the Tribology of Pure/Doped Diamond-like Carbon Coatings and Ionic Liquids" Coatings,2024, 14,71.

[22] M. Soori, M. Asmael, " A Review of the Recent Development in Machining Parameter Optimization". Jordan Journal of Mechanical and Industrial Engineering, Vol. 16, No. 2, 2022 pp. 205–223. .

[23]P. Ning, "An adaptive scheduling method for resources in used automobile parts recycling". Jordan Journal of Mechanical and Industrial Engineering, Vol. 14, No. 1, 2020, pp. 53–60.